Available online at www.sciencedirect.com

ScienceDirect

Procedia Engineering 213 (2018) 549–570

Procedia Engineering

www.elsevier.com/locate/procedia

7th International Conference on Fatigue Design, Fatigue Design 2017, 29-30 November 2017, Senlis, France

Aluminium weld fatigue: From characterisation to design rules

Z.Tahir[a*], R.Aso[b], T.Yates[c] , M.Bell[d] & A.Muse[e]

[a,b,c,d & e] *Gestamp Chassis, Skerne road, DL5 6EP, UK*

Abstract

In suspension design, traditionally subframes and links are welded structures, with one of the main design criteria being fatigue. Better understanding, correlation and correct design rules are vital to ensure safety and avoid over design that can lead to a reduction in competitiveness.

A known mesh modelling T-joint SN method is used to design the welds and is mainly driven from standards used for thicker panels seen in the construction and ship building industry.

To consider the thin sheet designs largely seen in automotive, Volvo & nCode have developed a new method based on structural stress and is known to be mesh insensitive. However, new difficulties emerged due to the clear separation between the membrane and bending behaviour needed for stress recovery. Specific tests need to be defined to ensure correct characterisation.

Gestamp has generated a new standard of design rules to ensure correlation in Weld-Ends and in Mid-Weld cracks and correct toe position definition to ensure accurate stress recovery, and give more beneficial input to process by better defining the weld torch position. New test specimens have been developed and intensive testing carried out to fully characterise the bending and tension behaviour and reduce the gap in predictions between Lap Weld and Fillet Weld. This methodology has been successfully used in suspension designs with high confidence and correlation.

These design rules have been used in conjunction with studying the effect of weld process and sequence on fatigue performance. Controlled distortion subframes, against high distortion subframes, have been tested to capture the benefit by reducing the fit-up gaps. Residual stresses are still a grey zone for Gestamp and further work is needed to better understand the effect.

Peer-review under responsibility of the scientific committee of the 7th International Conference on Fatigue Design.

Keywords: Aluminium, fatigue, welded joints, CAE SeamWeld, testing and distortion

1. Introduction

With the increase demand for reduction of weight and cost in the automotive industry, defining and correlating the design rules is becoming key to ensure accurate predictions in terms of fatigue performance to eliminate over-engineering. There is a clear correlation between robustness and accuracy of CAE (FEM) predictions and reduction

1877-7058 © 2018 The Authors. Published by Elsevier Ltd.
Peer-review under responsibility of the scientific committee of the 7th International Conference on Fatigue Design.
10.1016/j.proeng.2018.02.051

in cost and weight. Aluminium is seeing more widespread use in the automotive sector to reduce the weight and this drives a need to define new design rules and weld process control to ensure quality and safety.

Critical to defining these design rules is the analysis of the limits of the current methods and develop a range of testing to correlate all the predictions. Controlling the process and especially weld distortion is more important when dealing with aluminium due to high thermal conductivity and coefficient of thermal expansion which leads to larger heat affected zones and higher distortion compared to steel. In addition, penetration and fit-up gap have more effect compared to those seen in welding steel.

2. Nomenclature

σ_s	Structural stress
$\sigma_{nominal}$	Nominal stress
σ_m	Membrane stress
σ_b	Bending stress
σ_{weld}	Weld stress
f_x	Normal force to weld toe
m_y	Moment around weld toe axis
t	Thickness
r	Bending ratio
I	Bending interpolation function
m	Crack propagation exponent
r_{th}	Bending ratio threshold
$\Delta\sigma_b$	Bending stress range
$\Delta\sigma_m$	Membrane stress range
N	Number of cycles
a_b	Bending stress range intercept
a_m	Membrane tress range intercept
c_b	Bending fatigue strength exponent
c_m	Membrane fatigue strength exponent
a_s	Structural stress range intercept
c_s	Structural fatigue strength exponent
CAE	Computer aided engineering and corresponds to finite element method (FEM)
SE	Standard error
q	Inverse normal distribution for 99% probability
R	Testing ratio
UTS	Ultimate Tensile Strength
b_t	Measured weld bead thickness
h	Hypothetical weld bead thickness

3. SeamWeld fatigue approach

Traditionally, a T-joint mesh based on a single SN curve has been used to design chassis welded structures. This conservative approach leads to over design and heavier structures compromising the weight saving targets.

The stress distribution in weld according to ASME Boiler and Pressure Vessel Code [1] is a combination of membrane, bending and nonlinear stress as in eq.1.

$$\sigma_{weld} = \sigma_m + \sigma_b + \sigma_{nl} \quad (1)$$

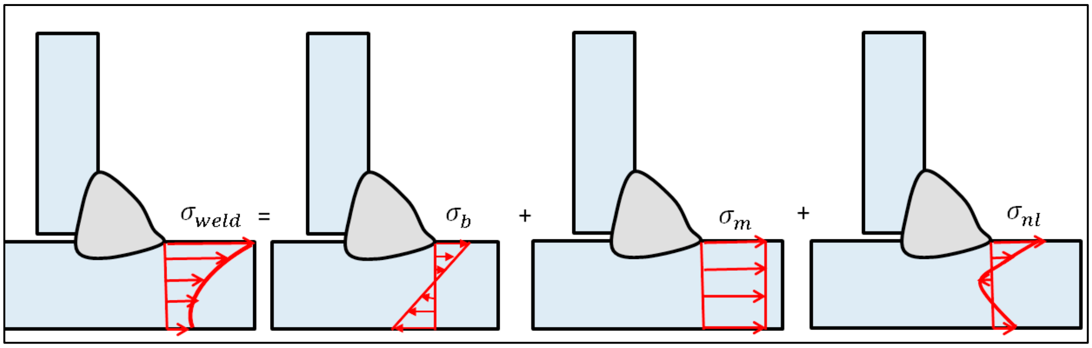

Fig.1. Weld structural stress distribution

The nonlinear stress σ_{nl} due to the local shape of the weld is studied in detail (see section 4.2) and considered by offsetting the fatigue curves identified in testing (implicitly including the notch on the S-N curve) instead of the considerable effort of notch modelling with very detailed 3D meshes which are not suitable for a robust design approach.

Volvo / nCode have implemented this approach based on structural stress and a clear separation between membrane and bending behaviour at the weld toe (Fig. 2). The structural stress (notch factor is not considered) is characterised as follows:

$$\sigma_s = \sigma_m + \sigma_b = \frac{f_x}{t} + \frac{6m_y}{t^2} \quad (2)$$

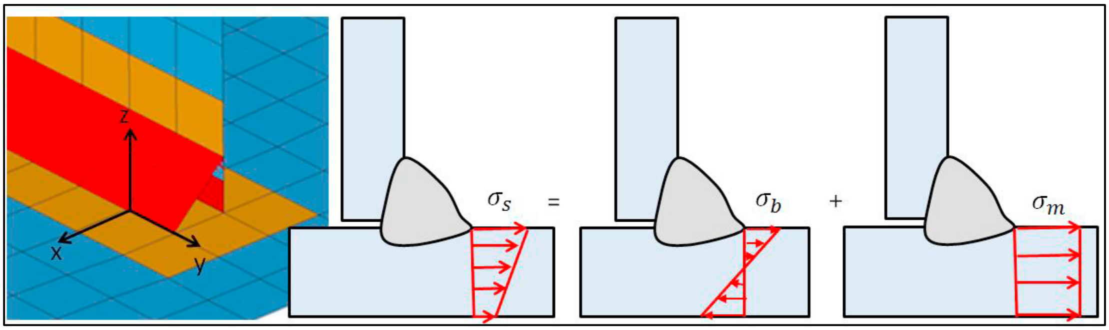

Fig.2. Weld toe axis definition and structural stress

A master SN curve is obtained by combining both bending and membrane SN curves. A bending ratio is defined to capture the actual stress state. An interpolation parameter I(r) is obtained from fracture mechanics based on Paris law to ensure correct stress recovery [2, 3].

The equations obtained for crack exponent propagation m=4 [4] are shown below:

$$I(r)^{\frac{1}{m}} = 12.64r^3 - 8.5153r^2 + 1.7653r + 5.0484 \quad (3)$$

$$r = \frac{\sigma_b}{\sigma_m + \sigma_b} \quad (4)$$

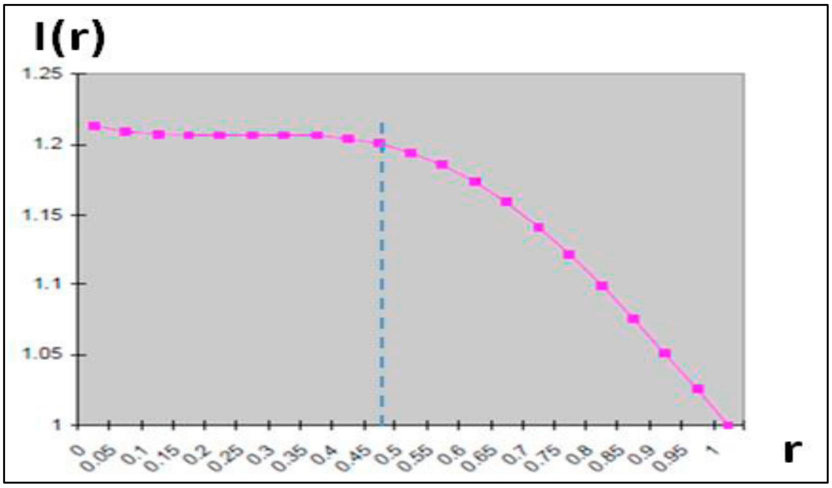

Fig.3. Bending ratio

Volvo and nCode have made further simplification by introducing a bi-linear approach which is used for the combined SN curve. Under the threshold $r_{th} \sim 0.5$, only the stiff curve is used and over, a linear combination is used as shown in Fig. 4.

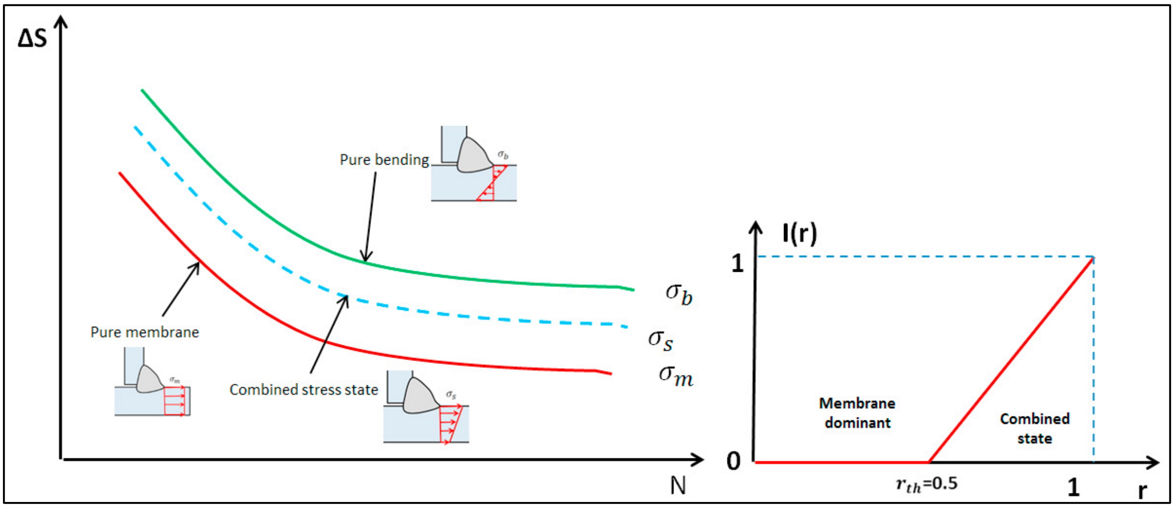

Fig.4. Master SN curve interpolation

Size effect and mean stress effect are considered using the FKM approach and reference thickness.

4. Fatigue design curve generation - Test/FEM

To ensure robust and correlated FEM (CAE) predictions, a range of testing has been developed to characterise the pure bending and pure membrane behaviour. A specific test is also generated to validate the bending ratio interpolation used to generate the master SN curve. The effects of penetration and weld ends are also studied in detail.

4.1. Crack detection methodology

To ensure accuracy in crack detection (visible 1mm to 2mm crack), a photographic detection methodology has been developed and compared to the standard “stiffness loss” approach.

A computer controlled camera was used to picture the expected crack weld area every 1k cycles and detect the initiation within 1k cycle error (worst case 10% from the min life of 10k cycles).

Fig.5. Crack initiation detection

The error based on stiffness approach is about **41%** and camera approach error is less than **5%.**

Specn #	Load Range (kN)	Frequency (Hz)	Cycles; Initiation(Stiffness loss)	Cycles; Initiation(camera)	GAP error Camera (%)	GAP error loss stiffness (%)
3	43.04	5	210,700	210,000	**-0.5%**	-0.3%
4	43.03	5	229,900	230,000	**-0.4%**	0.0%
5	43.03	5	129,100	128,350	**-0.8%**	-0.6%
26	33.03	5	388,500	388,900	**-0.3%**	0.1%
22	33.09	5	558,900	559,000	**-0.2%**	0.0%
16	27.04	5	1,361,700	1,201,050	**-0.1%**	-11.8%
25	27.04	5	1,281,900	1,280,000	**-0.1%**	-0.1%
20	60.04	5	54,800	34,000	**-2.9%**	**-38.0%**
21	60.04	5	51,800	32,000	**-3.1%**	**-38.2%**
24	50.03	5	118,400	69,800	**-1.4%**	**-41.0%**
17	50.04	5	103,100	72,000	**-1.4%**	**-30.2%**
18	36.18	5	564,000	400,000	**-0.3%**	**-29.1%**
14	36.04	5	715,100	716,000	**-0.1%**	0.1%
13	36.05	5	401,100	402,000	**-0.2%**	0.2%
9	40.05	5	342,400	342,000	**-0.3%**	-0.1%
15	40.05	5	312,200	312,000	**-0.3%**	-0.1%

Table 1. Crack initiation detection results

4.2. Nonlinear notch stress modelling strategy

As presented in equation 1, the nonlinear notch stress can be dealt with by two approaches:

- Use a detailed 3D FEM modelling of the weld to capture the local shape of the weld. This approach has a significant disadvantage of considerable effort on modelling and time consumption.
- Study the details of the shape of welds related to the Gestamp welding process using statistical analysis of the micro-sections and apply a notch offset identified from testing to the fatigue curves on the structural stress.

The notch stress offset is the delta between the local notch stresses and the structural stress as shown below:

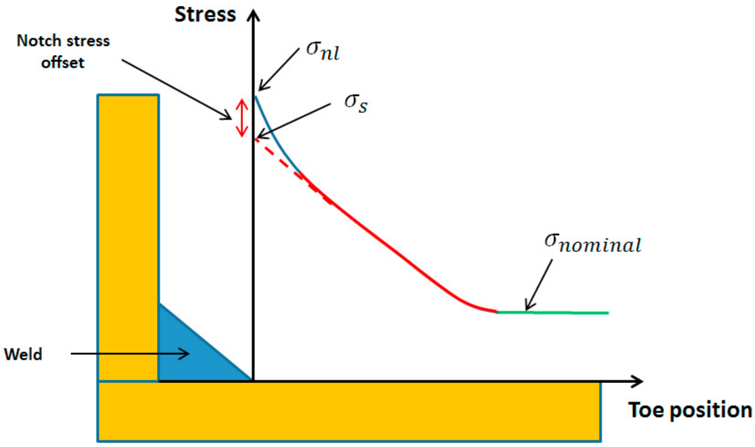

Fig.6. Notch offset definition and stress distribution

Different cut-sections have been done through different Gestamp welded products and the scope is reduced to one common shape.

Comparing hypothetical throat "h" with real throat "b_t" gives a measure of how convex/concave the weld is. A ratio close to 1 represents a straight "triangular" weld. A higher ratio corresponds to a more convex weld bead.

Fig.7. Weld shape definition

From a study of 460 fillet and 305 lap welds, a mean convex ratio of 0.95 with a standard deviation of 0.16 was found. This leads to a nearly triangular and consistent shape. Therefore, this will ensure little variation on the offset factor related to notch stress.

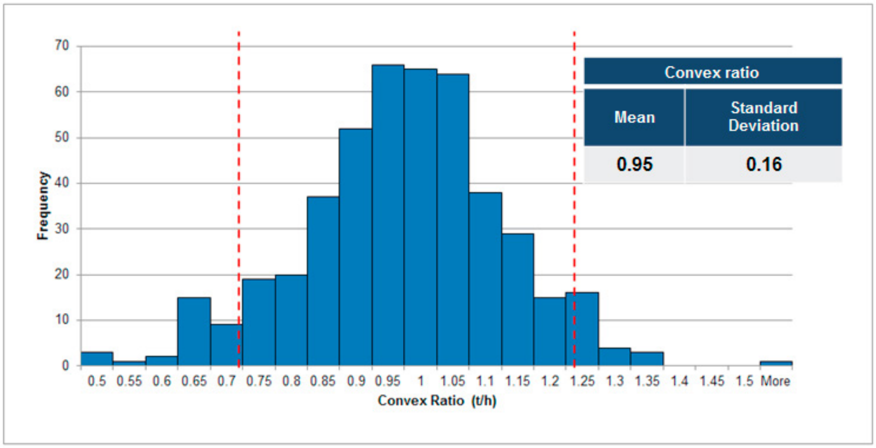

Fig.8. Convex ratio distribution

4.3. Pure Bending and pure membrane design curves

Pure tension (membrane) and bending testing procedure has been implemented.

$\Delta\sigma_b = a_b \times N^{c_b}$ ……………………… (6)
$\Delta\sigma_m = a_m \times N^{c_m}$……………………… (7)

Linear regression is used to generate the fatigue parameters for 50% survival.

$\log N = B \times log\, \Delta\sigma + A$……………………… (8)
Where $B = \frac{1}{c}$ and $A = -\frac{1}{c} \times log\, a$, or $c = \frac{1}{B}$ and $a = 10^{-(\frac{A}{B})}$

SN curves representing 1% and 99% of survival are obtained as follows:

99% survival: $logN_f = B \times log\, \Delta\sigma + A - q \times SE$; $\Delta\sigma = a_{99\%} \times N^c$ ……………………… (9)
1% survival: $logN_f = B \times log\, \Delta\sigma + A + q \times SE$; $\Delta\sigma = a_{1\%} \times N^c$ ……………………… (10)

Where SE is the standard error of log (N) obtained from regression analysis; q is the inverse normal distribution for 99% probability with mean and standard deviation values being 0 and 1 respectively.

Both EndWeld and MidWeld cracks have been characterised under various loading conditions; tension, lateral bending and axial bending.

Different grade joints used in designing chassis (6063-T66/6063-T66, 6063-T66/5754-H22, A356-T6/5754-H22, 6082-T6/5754-H22) were tested to capture variation from a variety of aluminium production technologies (stamping, extrusion, hydroforming and casting). All test specimens used weld wire 4043.

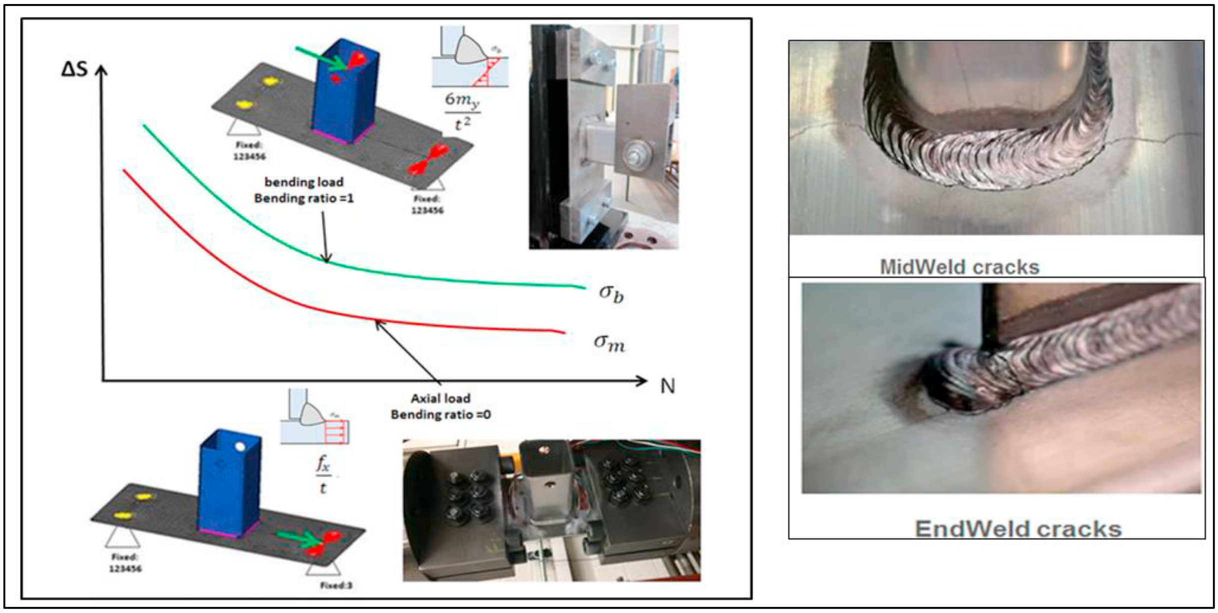

Fig.9. Tension and bending test procedure

Specimens with different gaps and different levels of penetration were built to study their effect on fatigue and build correct scatter on the design curves. This also includes toe and root cracks.

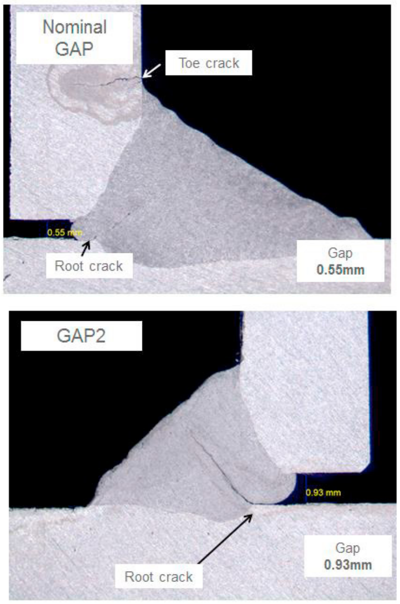

Fig.10. Gap and crack location study

Correlations between finite elements method (CAE) and testing are presented below (**test ratio R=-1**). Stress values are normalised.

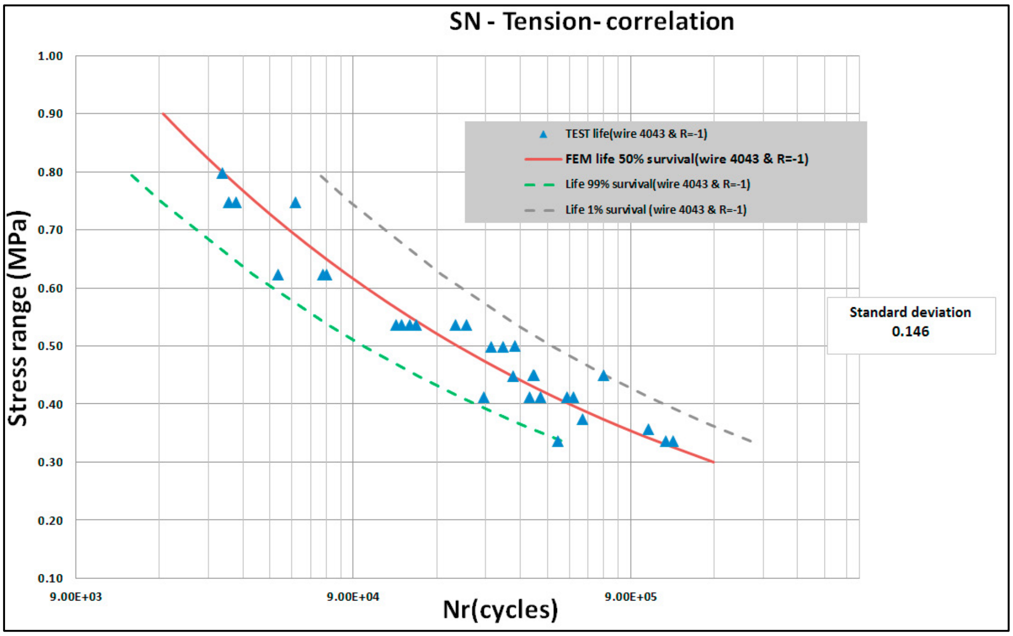

Fig.11. Membrane testing correlation

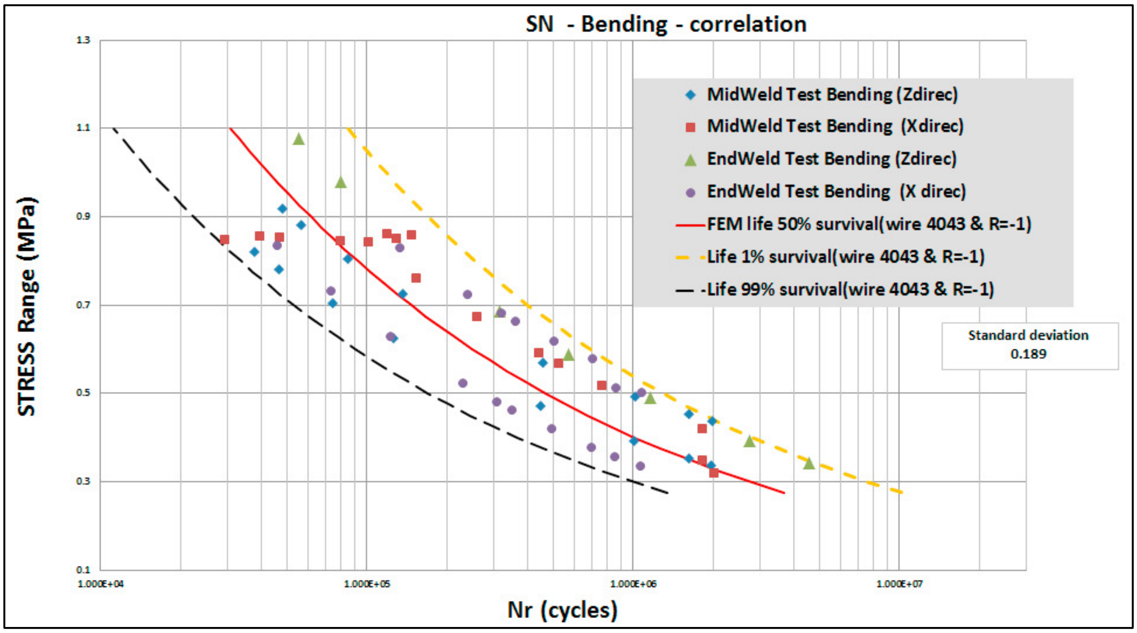

Fig.12. Bending testing correlation

The inverse identification developed allows Gestamp to generate fitted design curves with the highest confidence on mesh density representing Gestamp process weld geometry.

4.4. Combined Bending / membrane validation

As previously stated, the SeamWeld method relies on the interpolation ratio between the pure membrane and pure bending. A test has been generated with the combined stress state to validate the approach.

A flat welded lap joint generates a combined stress state (**bending ratio ~0.7**) due to the offset between the plates.

Typical stress distribution and deformation on single lap joint is shown below:

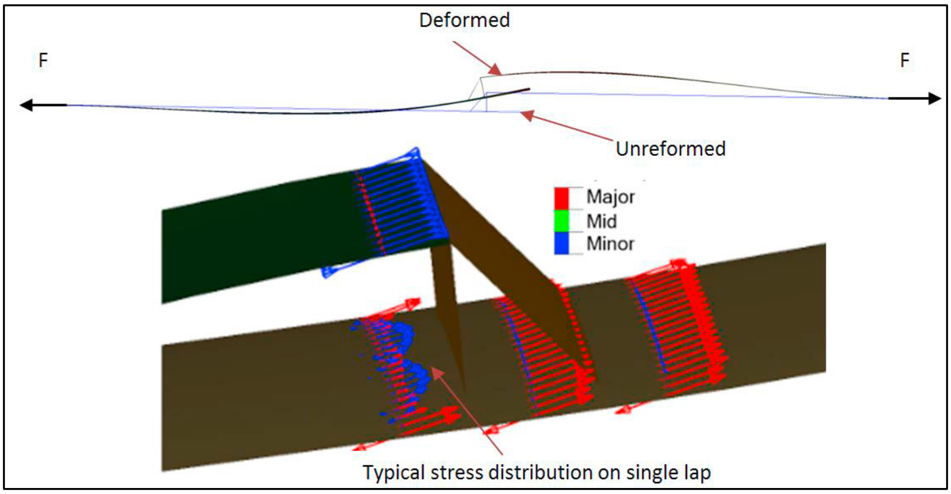

Fig.13. Combined test deformation and stress distribution

The interpolation is based on the following equations:

$$a_s = a_m + (a_b - a_m) \times I \quad (11)$$

$$I = \frac{r - r_{th}}{1 - r_{th}} \quad (12)$$

$$\Delta\sigma_s = a_s \times N^{c_s} \quad (13)$$

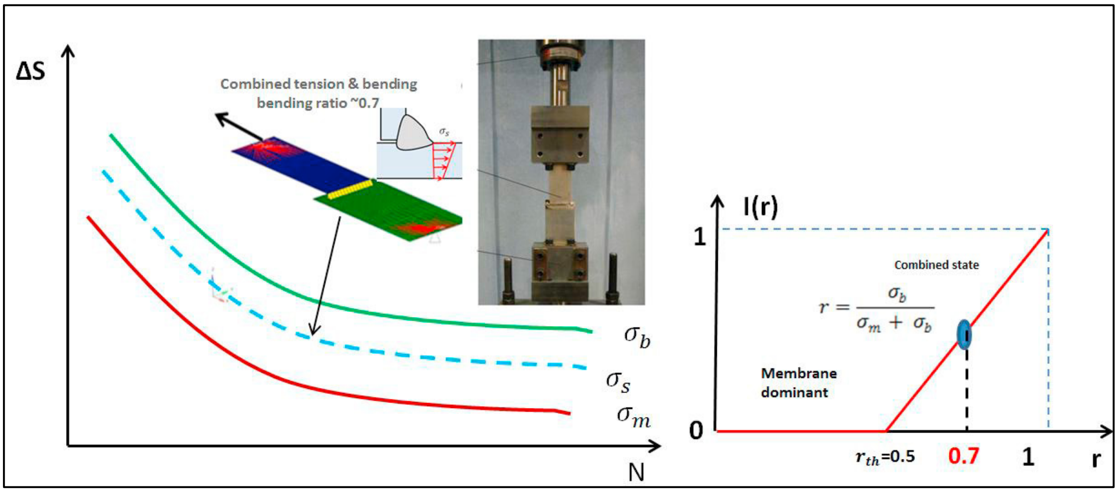

Fig.14. Combined test

The results obtained clearly show a good correlation between the CAE results and test results.

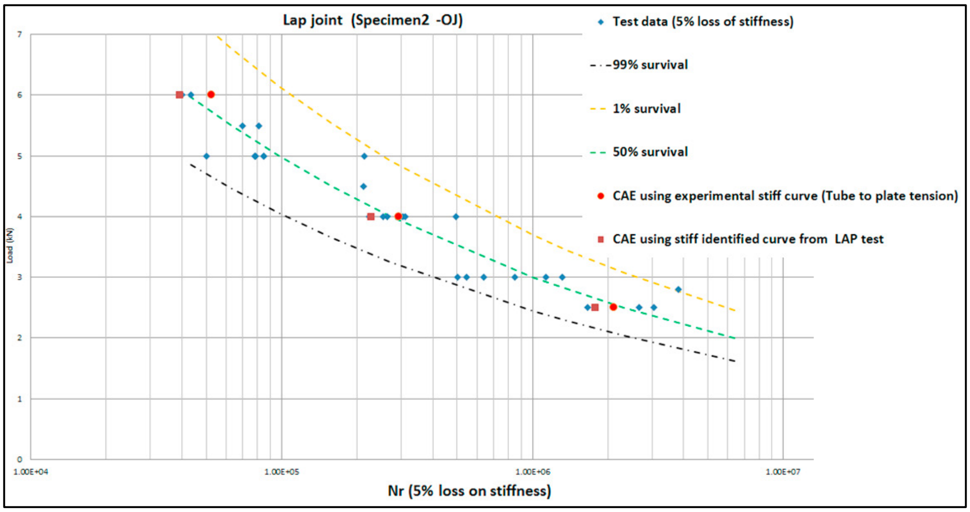

Fig.15. Combined test results

The CAE membrane curve identified from the combined test (brown points), converges to that identified by pure tension (red points). Both points are within the 50% survival of the test points which validates the interpolation approach.

4.5. Reliability analysis on SN design curve

To better capture the dispersion on characterisation, a reliability analysis was done to ensure the 50% design curve is calculated from a sufficient number of test points. The design target is between **1E5** and **4E5** cycles

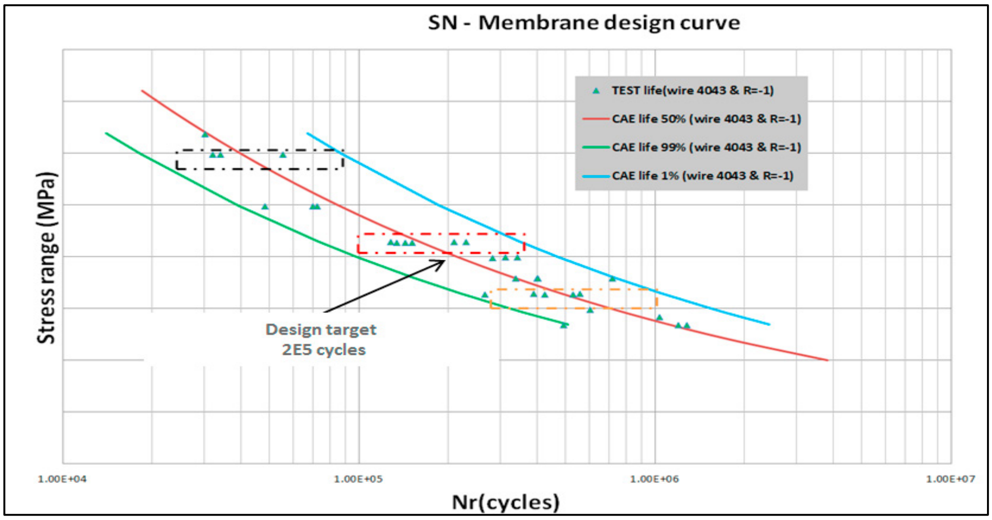

Fig.16. Tension points dispersion

A Weibull distribution curve was fitted to the population around the design target and the 50% survival curve is compared to a hypothetical mean value, if more samples were tested.

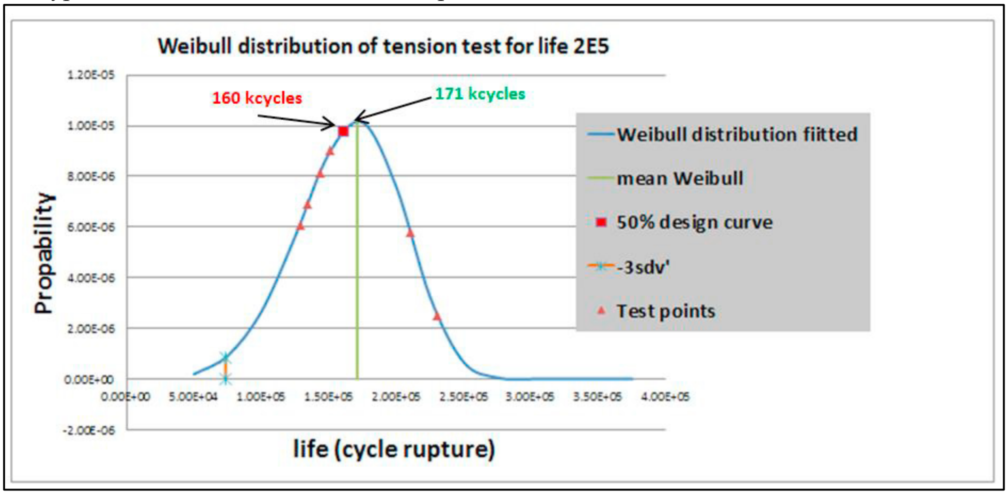

Fig.17. Weibull analysis

As beta (4.854) is higher than 3.5, Weibull distribution converges to normal distribution.

The 50% design curve calculated using regression [Log (N) =a*Log(S) +b] on total population (30 specimens) is 160k cycles in the design target and is comparable to the mean value from Weibull distribution ~171k cycles.

4.6. CAE stress recovery comparison – T-joint / SeamWeld

Traditionally, a known mesh modelling T-joint SN / EN method is used to design the welds. This consists of representing the weld with one single vertical shell element connecting the two panels modelled with shell elements. The difficulty with this method is how to correctly capture the position of weld toe and also how to deal with weld ends.

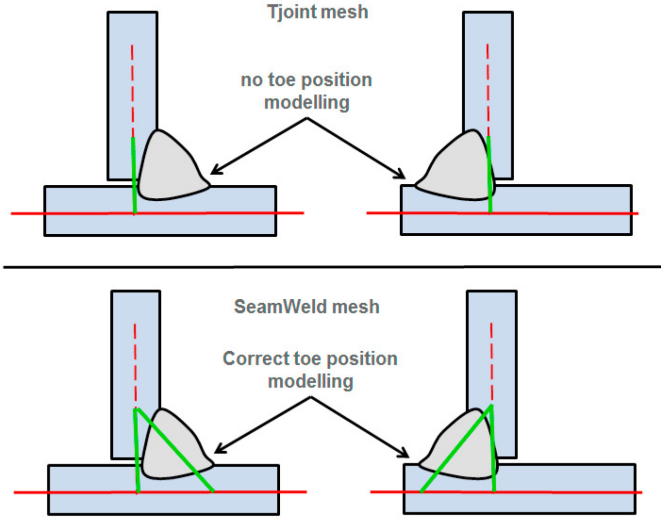

Fig.18. Modelling differences between SeamWeld and T-joint

The stiffness of the joint is better captured and the stress recovery is more consistent using the SeamWeld method. This allows studies into the effect of the panel thickness on the toe position and generates the correct design rules for thin sheet metal pressing, thick extrusions and thick castings

A statistical analysis is done through cut-sections to determine the length of the weld leg and define the mesh density **L_{elem}** to fit the fatigue curves. Normal distribution gives **95%** probability that a given weld will be larger than **L_{elem}**

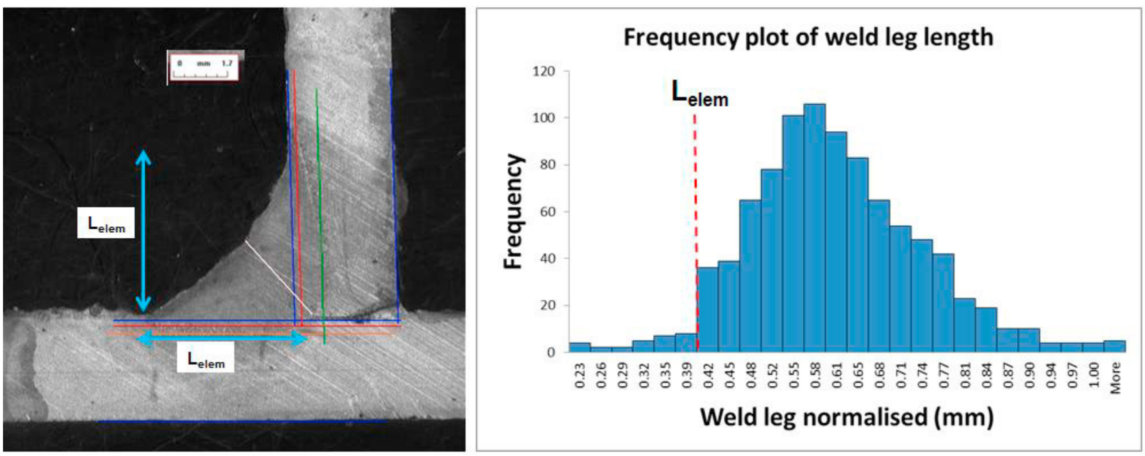

Fig.19. Statistical analysis of weld length

Using a mesh standard based on **L_{elem}**, design curves have been generated and fully correlated using the Gestamp Standard below.

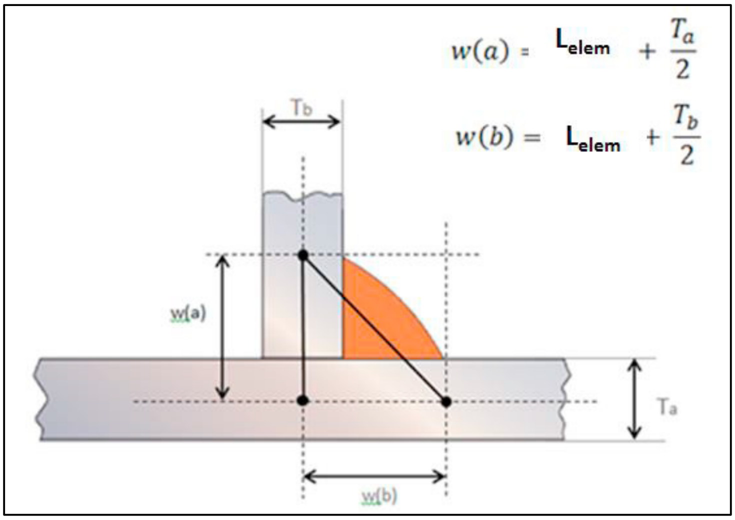

Fig.20. Finite elements mesh standard

The methodology ensures avoiding stress recovery variation due to mesh size.

The sensitivity study is shown below using the design curves presented previously:

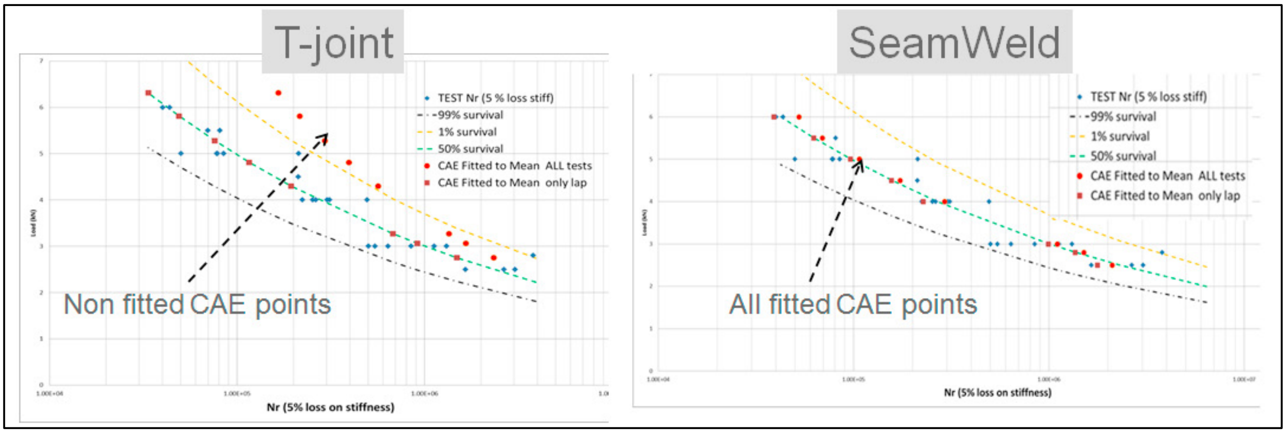

Fig.21. T-joint/SeamWeld comparison

The T-joint method needs different SN parameters for each geometry and load directions to be able to fit in CAE all the test points, whereas the SeamWeld approach needs only one CAE master SN curve to fit all the test points.

4.7. Mean stress effect validation

The dominant factor on fatigue damage is stress range. It is also influenced by the mean stress of each cycle. Different methods exist to model the effect of mean stress. FKM approach was used in this study. It uses four regimes that define the sensitivity to mean stress.

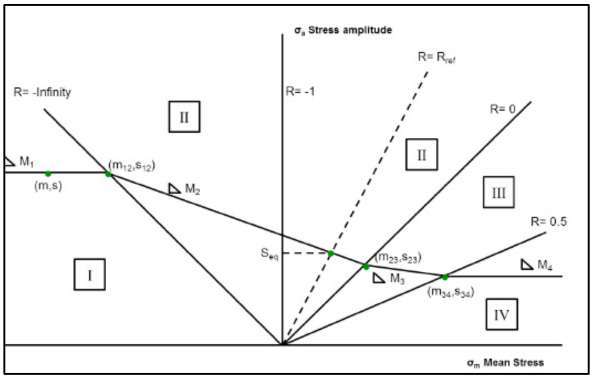

Fig.22. FKM approach

The four factors M_i are obtained by testing or estimated using the following equations:

$M_1 = 0,\ M_2 = -M_\sigma,\ M_3 = \frac{-M_\sigma}{3},\ M_4 = 0$ .... (14)

Where: M_σ is a function of UTS.

However, for welded joints, different grades are joined and the structure of the weld itself is affected by the contribution of joined parts (UTS value will depend on the grades of the welded panels). It becomes obvious for design robustness to identify M_σ through testing.

The design curves developed and presented in the previous paragraphs are for fully reversed loading **R=-1**. A lap joint specimen is designed to analyse the mean stress effect (**R=0.1**). Different types of End Welds are analysed (normal length, short welds and run on/off)

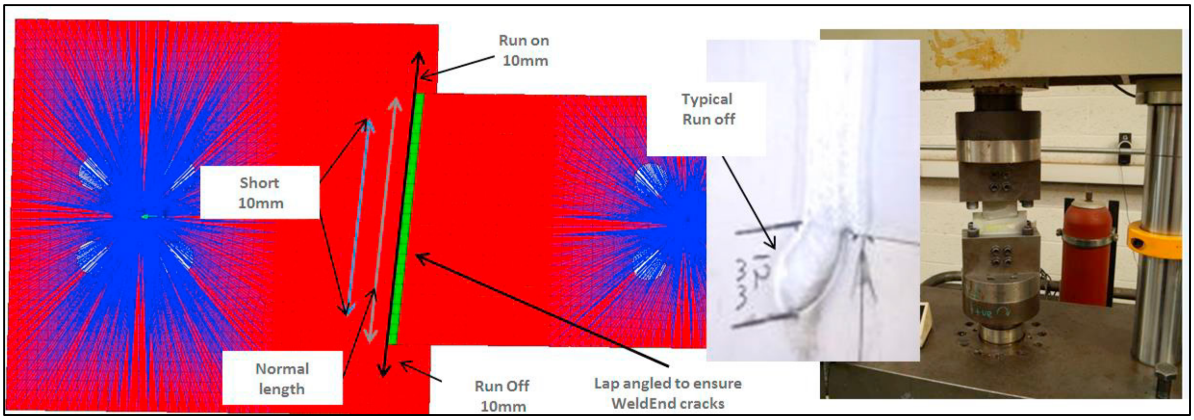

Fig.23. Mean stress / WeldEnd test

Different joints with different material grades were built using the 4043 wire to ensure to capture the grade variation.

The results obtained are shown below:

Sample #	Weld status	Applied forces (kN)	Jojnt type	Test failure (k cycles)	Test 50% (k cycles)	FEM 50% (k cycles)	Diffrence (%)
1	Normal	1.15 / 11.5 (R=0.1)	5754-H22/5754-H22 LAP inclined	69.6	56.4	58.4	3.5%
2				42.9			
3				56.5			
4				56.5			
5	Short			15.3	21.0	19.5	-7.7%
8				19.6			
7				22.6			
8				26.5			
9	Run on / off			66.5	61.8	**	NA
10				43.9			
11				62.0			
12				74.7			
1	Normal	1.15 / 11.5 (R=0.1)	5754-H22/A356-T6 LAP not inclined	19.9	44.0	42.6	-3.3%
2				54.8			
3				56.4			
4				45.0			
5	Normal	0.85/8.5 (R=0.1)		155.0	138.4	152.3	9.1%
6				121.4			
7				134.8			
8				172.4			
9				108.5			

Table 2. Mean stress/WeldEnd - Test/FEM results

The identified M_σ gives a very good correlation between test and finite elements results for different weld conditions. The maximum error between tests and FEM is less than **10%.** It is important to note that run on/off helps to avoid shortened welds and ensure effective weld length.

Investigation is ongoing to understand how to model the run on/off in CAE.

However, a good control of the weld parameters is needed to avoid burning the edges and initiating root/bead cracks defects.

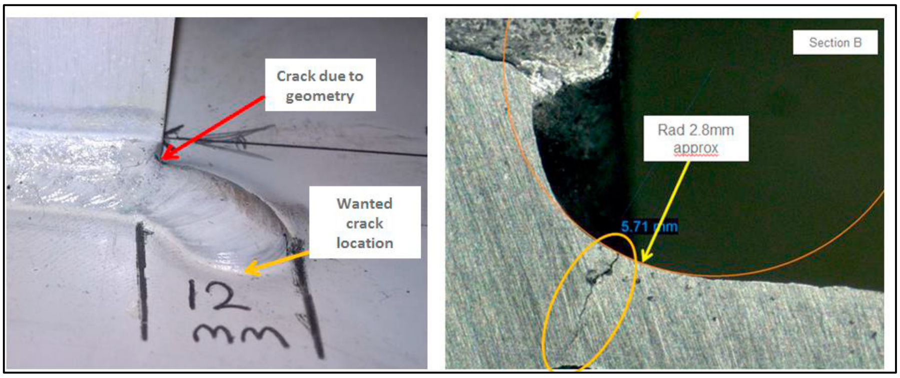

Fig.24. Weld defect crack

5. Correlation on subframes / suspensions

Correlation achieved on complex subframe assemblies using the design standards are presented below.

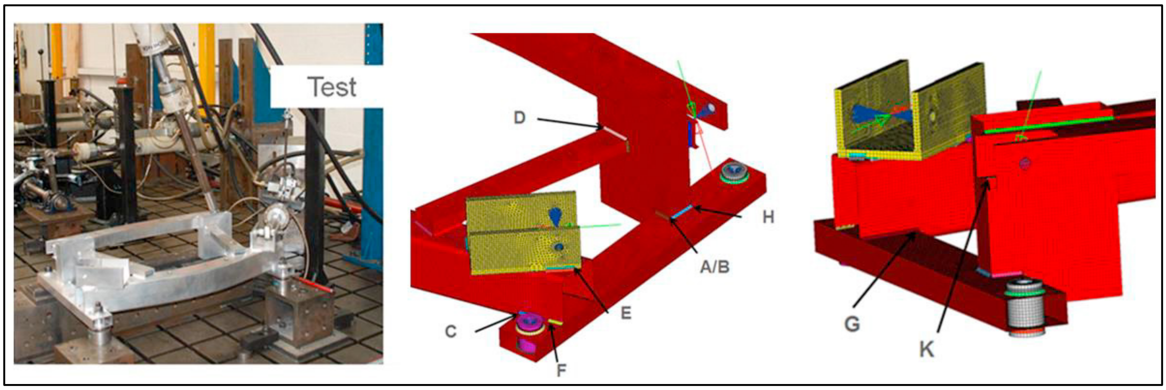

Fig.25. Subframe assembly testing

The results obtained for 5 subframes tested are shown below:

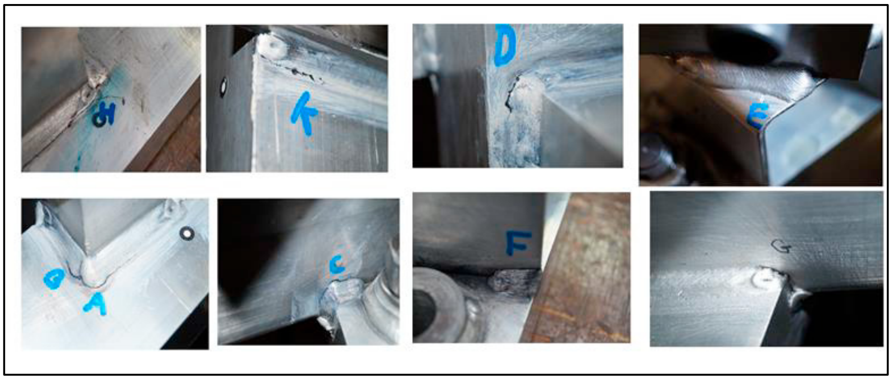

Fig.26. Subframe testing cracks

As seen below, there is good correlation obtained in the majority of locations.

Crack	Test no AYC-2326	Test no AYC-2492	Test no AYC-2498	Test no AYC-2771	Test no AYC-2804	Test mean (50%)	FEM (50%)	Test (99% survival)	FEM (99% survival)
A	16.0%	12.0%	13.0%	9.0%	20.0%	14.0%	9.0%	4.3%	2.2%
B	16.0%	16.0%	no crack	10.0%	30.0%	18.0%	26.0%	9.5%	7.9%
C	16.0%	30.0%	50.0%	20.0%	30.0%	29.2%	22.1%	13.6%	6.7%
D	33.0%	no crack	no crack	20.0%	no crack	26.5%	20.0%	11.8%	5.0%
E*	NA	NA	NA	NA	NA	NA	NA	NA	NA
F*	NA	NA	NA	NA	NA	NA	NA	NA	NA
G	no crack	no crack	no crack	60.0%	no crack	**	121.0%	60.0%	38.7%
H	16.0%	15.0%	40.0%	70.0%	30.0%	34.2%	19.8%	23.2%	5.2%
K	no crack	no crack	no crack	100.0%	no crack	**	120.0%	100.0%	39.4%

Table 3. Test / FEM results & correlation on subframe

* These locations are parent /edge material cracks and not weld joints
** No mean definition, only 1 of 5 subframes cracked in these locations.

6. Welding distortion effect on fatigue

Most chassis parts in the automotive industry are welded parts. Distortion is introduced due to the heating/cooling cycle of the welding process. The resulting deformation leads to quality issues such as tolerances and weld performance decrease related to poor fit-up and residual stresses.
This issue becomes even more critical when designing and manufacturing aluminium structures due to high thermal conductivity and coefficient of thermal expansion which leads to larger heat affected zones and higher distortion compared to steel.
Gestamp has developed a weld sequence optimiser, Optimised weld Parameters for Tolerance Improved Components (OPTIC) to achieve effective distortion reduction in prototype and production manufacturing [5, 6].

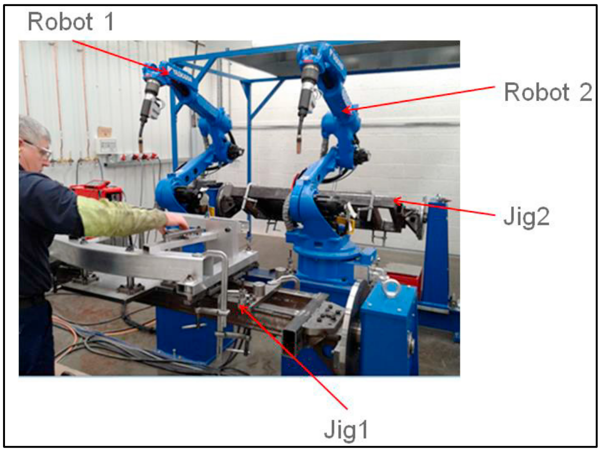

Fig.27. Subframe building

To capture the effect of distortion on chassis structures, multiple subframes were manufactured using the OPTIC tool. Both the optimised and worst weld sequence subframes were 3D scanned using GOM – ATOS Compact Scan and distortion in the hardpoints measured using CMM and compared directly to the CAE results. This phase is important to ensure fatigue testing on subframes with high and low distortion.

Hard Points Node	Magnitude (mm) Worst	Best	Magnitude reduction (mm)
1	0.00	0.00	0.00
2	4.16	2.30	1.86
3	2.66	2.28	0.38
4	2.42	2.18	0.24
5	2.57	2.26	0.31
6	2.59	2.32	0.28
7	3.38	2.89	0.49
8	3.27	2.80	0.48
9	3.56	2.92	0.64
10	3.45	2.86	0.59
11	3.32	2.67	0.65
12	3.65	2.36	1.29
15	2.71	1.93	0.78
16	4.19	3.61	0.59
17	3.28	2.48	0.80
18	3.14	3.74	-0.60
23	3.49	3.50	0.00
24	2.83	2.62	0.21
25	3.42	2.68	0.73
26	3.33	2.77	0.56

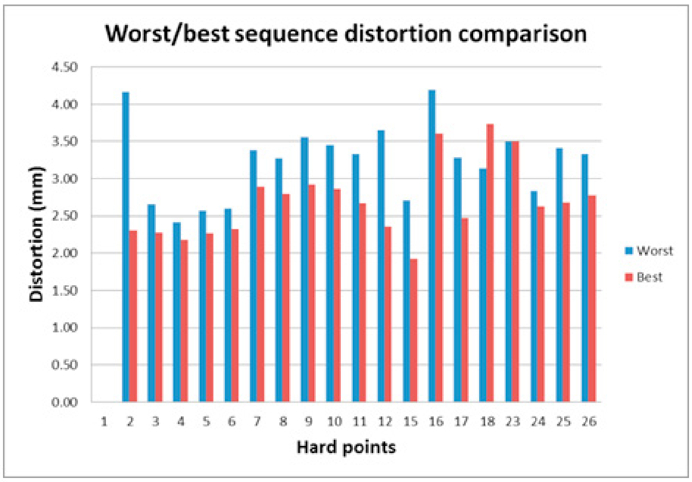

Fig.28. Distortion measurements

The optimised weld sequence clearly has lower distortion across almost all the hard points with a magnitude distortion reduction of 1.86 mm at hardpoint 2 and an average distortion reduction of 0.51 mm.

Fatigue testing has been carried out on 5 worst weld sequence frames (high distortion) and 5 optimised weld sequence frames (low distortion).

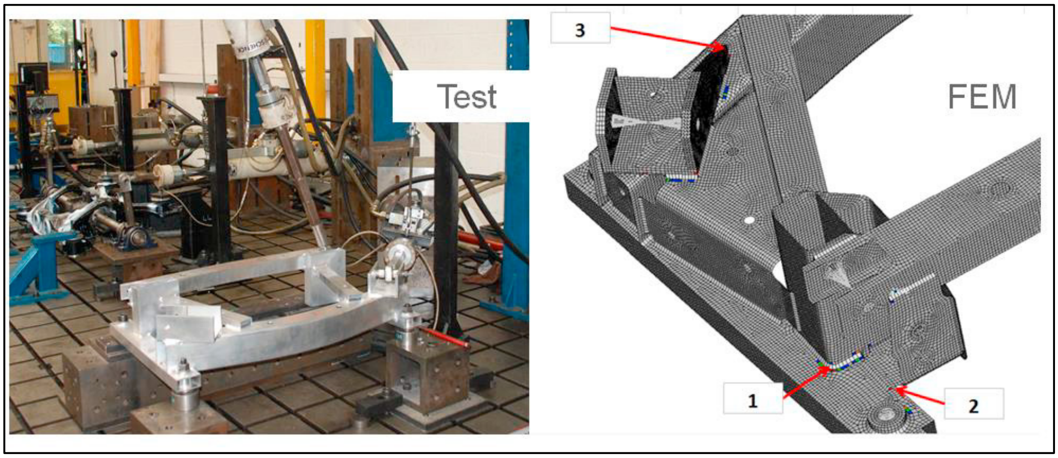

Fig.29. Subframe testing

The subframes are designed to achieve lives less than 100 kcycles (100%) on purpose, to be able to capture the benefit of the increasing lives from less distortion in relatively short time tests (run-out is 200 kcycles). Results for two frames are already available and testing is ongoing to finish the three remaining frames for each condition.

		Worst sequence		Best sequence		
Crack	CAE Target	Test AYC-2873	Test AYC-2907	Test AYC-2846	Test AYC-3012	increase on life
1	94.4%	40.0%	68.0%	190.0%	no crack	4.75
2	38.0%	60.0%	40.0%	no crack	no crack	>4
3	74.0%	110.0%	30.0%	180.0%	no crack	6.00

Table 4. Subframe testing results

The increase in life for location 1 is **475**% and for location 3 is **600**%. For location 2, no crack was obtained with the low distortion frame. As can be seen in the figure below, the optimised sequence provides a consistent and parallel fit-up between the two components.

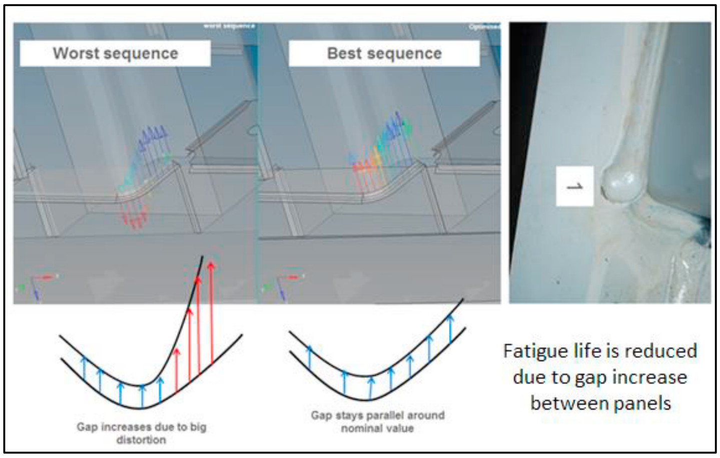

Fig.30. Crack 1

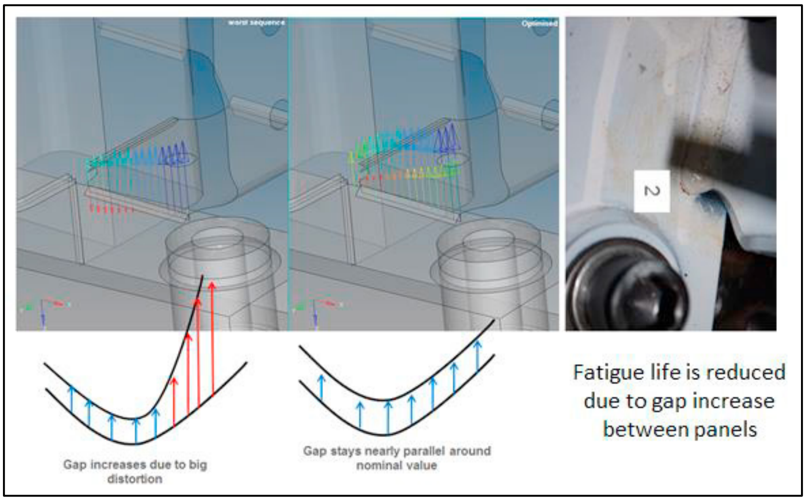

Fig.31. Crack 2

The effect of fit up gap on weld bead features that can affect fatigue performance was investigated using a wedge gap test coupon set up as shown below.

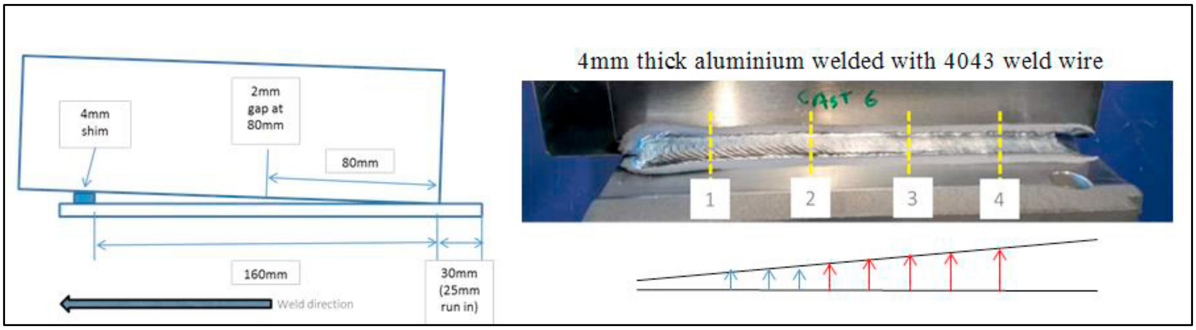

Fig.32. Weld gap effect test

Sections taken at intervals along the weld show the effect of a steadily increasing gap. The evolution of the weld profile can be seen below.

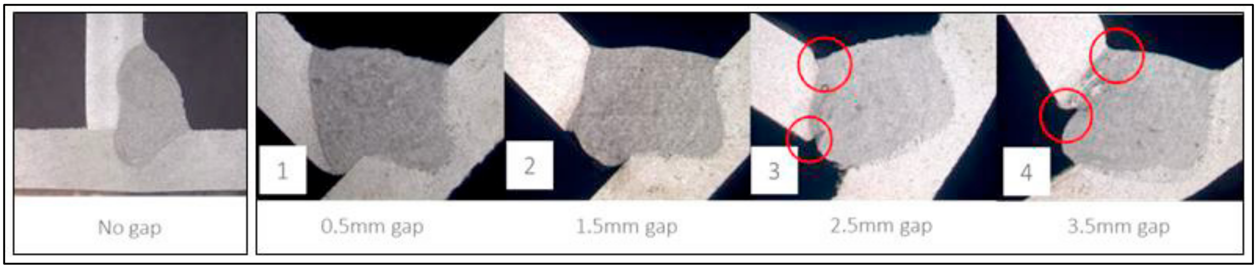

Fig.33. Gap effect on weld shape

As the gap increases the weld penetrates deeper into the space between the attachment and the lower panel. At some point between 0.5 and 1.5mm gap the weld fully occupies the gap. Shrinkage of this material is a driver towards increased distortion and residual stress.

These effects are greater with aluminium compared to steel due to aluminium's much higher coefficient of thermal expansion. Above 1.5mm, the gap begins to cause undesirable notches at the root profile and undercut at the weld toe (red circles in the pictures above).

Residuals stresses are not analysed yet in this study as the shrinkage method is not suitable for stress recovery. Full thermo-mechanical-metallurgical approach will be investigated.

7. Conclusion

Using a stiffness loss approach by itself (5% to 20% drop on load) is not always suitable due to potential error of 41%. However combined with photographic detection, the error on initiation detection is less than 5%.

Due to consistency of the weld shape, defining an offset on fatigue curve is validated and gives an advantage in term of robustness and simplicity of design iterations by avoiding a need to build very accurate 3D models of the notches.

Different geometries and configuration representing Gestamp designs have been tested to generate the required single design curves. Use of bending ratio interpolation to build the master design curve has been validated by using the combined tension / bending lap weld test.

The advantage of the SeamWeld approach has been shown through stress recovery consistence compared to T-joint method and through very good correlation with complex geometries and assemblies.

Weld distortion has a big impact on aluminium weld fatigue due to high thermal conductivity and coefficient of thermal expansion. Controlling the fit-up gaps led to increased life in the same location of over 400%.

It is clearly shown in this study that understanding all the parameters related to welding aluminium is vital to better defining the correct design rules.

References

[1] The American Society of Mechanical Engineers. ASME Boiler and Pressure Vessel Code Section VIII Division 2 Part 5: Design by Analysis Requirement; ASME: New York, NY, USA, 2007

[2] P. Heyes, Fatigue Analysis of Welded Structures Using nCode DesignLife, - HBM UK Ltd, Altair EHTC, Versailles, Oct 27-29 2010

[3] Y. Liu et al, Evaluation Model of Aluminium Alloy Welded Joint Low-Cycle Fatigue Data Based on Information Entropy, Entropy 2017, 19, 37; doi:10.3390/e19010037

[4] DesignLife Theory Guide, HBM United Kingdom Limited, 2014.

[5] Z. Tahir, R.Aso & W. McCavanagh, Weld Distortion Optimisation, NAFEMS UK Conference 2016, Telford, UK

[6] A.Chapple, Z. Tahir, F.Jardine, Weld Distortion Optimisation using HyperStudy, the 8th UK Altair Technology Conference 2013

Bibliography

S. Beretta and G. Sala, Fatigue Strength of Welded Lap Joints, Politecnico di Milano,

P. Selvakumar, J. K.Hong, Robust Mesh Insensitive Structural Stress Method For Fatigue Analysis of Welded Structures, Battelle India Pvt.Ltd.- Pune-411057, India, Centre for Welded Structures Research, Battelle, Columbus - OH 43201-2693, USA

T. Marin, G. Nicoletto, Fatigue design of welded joints using the finite element method and the 2007 ASME Div. 2 Master curve, University of Parma, Department of Industrial Engineering, Italy (Frattura ed Integrità Strutturale, 9 (2009) 76 - 84; DOI: 10.3221/IGF-ESIS.09.08)

T. Mann, Fatigue assessment methods for welded structures and their application to aluminium T-joints, Norwegian University of Science and Technology, Trondheim, Norway

V. Blanchot, calcul des soudures en fatigue, INSA Toulouse, France

Tr. E. Haibach, Analytical Strength Assessment of Components in Mechanical Engineering, 2003

S.J Maddox, Fatigue International Journal of Fatigue, Review of fatigue assessment procedures for welded aluminium structures